SciEn

Proceedings of 8th International Conference on Mechanical, Industrial and Energy Engineering 2024
02-04 January, 2025, Khulna, BANGLADESH

SciEn Conference Series: Engineering Vol. 3, 2025, pp 96-101 https://doi.org/10.38032/sesc.2025.3.21

Verification and Validation of the Added Resistance of a Container Ship in Head Waves using Computational Fluid Dynamics Technique

Md. Golam Kibria[1] and Md. Mashiur Rahaman[2,]*

[1]Offshore and Marine Engineering Ltd., Dhaka, Bangladesh
[2]Department of Naval Architecture and Marine Engineering, Bangladesh University of Engineering and Technology, Dhaka, Bangladesh

ABSTRACT

Prediction of resistance in a seaway is always a challenging task for a naval architect. It is necessary to evaluate the performance of sea-going vessels in the earlier stage of design for both sea-keeping and economic perspectives of views. Traditionally required power is predicted based on calm water simulation with a predetermined allowance of (15-30%) of sea margin. This type of practice is totally reliant on experience and never represents the actual sea state. The present study evaluates the added resistance of a ship in a seaway at various wavelengths using RaNS based open-source Computational Fluid Dynamics solver OpenFOAM. The ship model was developed by the Korean Research Institute of Ship and Ocean Engineering and named as KRISO container ship of 3600 TEU. The experimental results of the hull are provided by NMRI (National Maritime Research Institute) in Tokyo CFD Workshop 2015. The current study begins with the validation of numerical results against experimental results. A systematic verification study based on grid size is further performed to evaluate the uncertainty present in numerical results. Finally, the added resistance coefficient is predicted for four different wavelengths at Froude number 0.26. It is seen from the computational results that the total resistance in the seaway increases with wave length and maximum resistance is found which is close to twice of calm water resistance in a situation where wave length is greater than ship length.

Keywords. Added resistance, sea margin, CFD, OpenFOAM, KRISO.

1. Introduction

Shipping industry plays a dominating role in merchant fleet by covering about 84.5 % of the international market. Container ships representing 16% of the world's merchant fleet (Equasis 2020) [1]are well known for the fast shipping of containerized cargo playing a vital role in the shipping industry. They have to operate in various sea conditions. So, the present study focuses on added resistance of container ships.

Several studies were done in the field of prediction of added resistance using both empirical and numerical methods. The first attempt to calculate the added resistance was made by T.H. Havelock (1937) [2]. He calculated the added resistance of ship in head wave by performing integration of longitudinal component of pressure distributed over hull. It is based on direct integration. The limitation of the method is that, results obtained from higher wave length to ship length ratio. It is based on near field method. There was another method to calculate the added resistance of ship named far field method. The method calculates added resistance of ship-based conservation of momentum theory was first introduced by Maruo (1960) [3]. It was based on potential theory, where the viscosity of water is neglected. He implemented a circular factor to calculate the added force due to wave. The limitation of the method is that it is applicable only for small amplitude waves. Gerristma and Beukelman (1972) [4] extended Maruo's (1960) method and used strip theory considering ship section as a circular section. They calculated the added resistance for each section and later integrated it. Drawback of the method is accurate prediction of added resistance is not possible due to circular section.With the rapid development of computational power, Computational Fluid Dynamic (CFD) codes are now popular for calculating added resistance of ship after the development of RaNS (Reynolds-averaged Navier–Stokes) equation. In year 2003, Orihara and Miyata [5] predicted added resistance of SR 108 hull using a RaNS based CFD solver WISDAM-X. They used overlapping grid method and discretize the governing equation using FVM (Finite Volume Method). Their results shows good agreement with experimental result. H.Islam and M.M. Rahaman et.al. (2019) [6] used potential flow based solver named as HydroStar and RaNS based solver named as SHIP_Motion to perform head wave simulation of KVLCC2 ship with a heave and pitch-free motion. Both of the solvers showed good accuracy with experimental results for heave and pitch motions but the potential flow-based solver showed a large error in drag force prediction. H. Islam and C. Guedes Soares (2020) [7] predicted the added resistance of the KVLCC2 ship using Open FOAM in head wave with 2 DOF (heave and pitch). Their study showed good results in longer waves though there was a large deviation in shorter wave lengths. In 2021 H.Q Nguyen et.al. [8] predicted the added resistance of KCS hull using five different wave lengths and compared the only mean value of resistance co-efficient with experimental results. They have conducted their study in commercial CFD solver Star CCM+.

The present research mainly evaluates the added resistance of KRISO container ship in head wave with 2 DOF (degree of freedom) heave and pitch-free motion using an open-source RaNS-based Computational Fluid Dynamics solver.

*Corresponding Author Email Address: mashiurrahaman@name.buet.ac.bd Published By: SciEn Publishing Group

2. Research Methodology

A Panama max 3600 TEU container ship named KCS is simulated in calm water and head wave conditions with heave and pitch-free motion. Both calm water and wave condition simulations are performed in OpenFOAM version 11. Initially, the calm water simulation is run at Froude number 0.26 then head wave simulations are run at the same Froude number with four different wavelengths and wave heights. Finally added resistance coefficient is calculated and the percentage of increase in resistance is predicted.

3. Ship model

The KCS ship model was developed by Korean Research Institute of Ship and Ocean Engineering widely used by the marine hydrodynamic researchers. It is benchmark modern container ship with a bulbous bow, flare above the waterline and pram type transom stern. A model appended with rudder has been considered for the current study. The principal particulars of the model are mentioned in Table 1. The profile view and body plan view have shown in Fig.1.

Table 1 Principal Particulars of KCS hull.

Specification	Symbol	Full Scale	Model Scale	Unit
Length between perpendiculars	L_{PP}	230.00	6.0702	[m]
Length of waterline	L_{WL}	232.50	6.1357	[m]
Maximum beam of waterline	B_{Max}	32.20	0.8498	[m]
Depth	D	19.00	0.5067	[m]
Draft	T	10.80	0.2850	[m]
Block Co-efficient	C_B	0.6505	0.651	--
Wetted surface area w/o rudder	S_W	9424.0	6.6177	[m^2]
Wetted surface area rudder	S_R	115.00	0.0801	[m^2]
Scale	λ	1:1	1:37.89	--

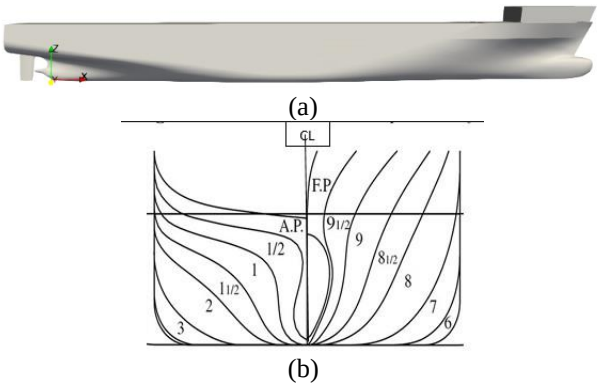

Fig.1 Profile view (a) and body plan (b) of KCS hull

4. Numerical method

The numerical model in Open FOAM is based on governing equations are continuity equation (1) and Navier Stoke's equation (2) for incompressible flow.

$$\nabla . v = 0 \tag{1}$$

$$\rho\left(\frac{\partial u}{\partial t} + u.\nabla u\right) = -\nabla p + \mu\nabla^2 u + \rho g \tag{2}$$

The governing equations are discretized using FVM (Finite Volume Method). The RaNS equation has been solved using an iterative PIMPLE algorithm which is the combination of PISO and SIMPLE algorithm. Two equations SST k-omega turbulence model have been used for turbulence energy and dissipation rate. To capture the water-air interface VOF (Volume of Fluid method) has been used. A rigid body motion solver has been applied to accommodate the motion of hull which is defined inside the dynamicMeshDict. In wave simulations, waveProperties dictionary has been used. Three-dimensional view of the computational domain is shown in below Fig. 2.

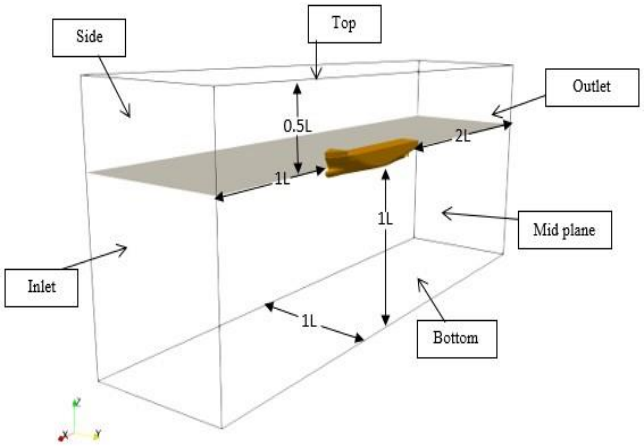

Fig.2 3D view of computational domain in x, y, z space

5. Boundary condition

The boundary conditions in head wave condition are different from calm water condition. The boundary condition in calm water condition and wave condition are mentioned in Table 2 and Table 3 respectively.

Table 2 Boundary condition in calm water condition.

Boundary	Velocity	Pressure
Inlet	fixedValue	fixedFluxPressure,
Outlet	outletPhaseMeanVelocity	zeroGradient
Hull	movingWallVelocity	zeroGradient
Sides	symmetryPlane	symmetryPlane
Bottom	symmetryPlane	symmetryPlane
Top	pressureInletOutletVelocity	totalPressure

Table 3 Boundary condition in wave condition.

Boundary	Velocity	Pressure
Inlet	waveVelocity	fixedFluxPressure
Outlet	outletPhaseMeanVelocity	zeroGradient
Hull	movingWallVelocity	zeroGradient
Sides	symmetryPlane	symmetryPlane
Bottom	symmetryPlane	symmetryPlane
Top	pressureInletOutletVelocity	totalPressure

Here, fixedValue means a constant value specified by the user end input, zeroGradient means no change with respect to time, waveVelocity defines velocity of wave, fixedFluxPressure sets the gradient of pressure to the specified by the flux on the velocity boundary condition. pressureInletOutletVelocity specifies velocity where pressure is defined, outletPhaseMeanVelocity adjusts the velocity such that causing the phase-fraction to adjust according to the mass flow rate. movingWallVelocity is the boundary condition for a wall type object moving with a constant velocity, symmetryPlane specifies no interaction with fluid flow. Details about this boundary condition are given in OpenFOAM user guide.

6. Computational resources

A desktop computer powered with Intel core i7 processor and 16 GB of ram has been used in the present study. It has taken about 50 sec of simulation time which is corresponding to 48 hours of physical time for calm water simulation. Head wave simulations are more resources consuming. The simulations are run up to 20 encountering period which corresponding to 120 to 240 hours of physical time depending of wave lengths.

7. Mesh generation

Two different mesh configurations have been used for calm water and wave condition simulations. Finer grid requires for wave condition for smooth propagation of wave. For calm water simulation inlet is placed 1 L_{pp} from the fore perpendicular, outlet is placed 2 L_{pp} from the aft perpendicular, side is placed 1 L_{pp} from the centerline, bottom of the domain is placed 1 L_{pp} from the free-surface and top of the domain is placed 0.5 L_{pp} from the free surface according to ITTC-2011 guide line. In head wave simulation the domain is generated according to the description provided by Alfaz Hossain et.al (2017) [9]. Inlet of the domain is placed 0.5 Lpp for short waves ($\lambda/L = 0.65, 0.85$) and 0.6 Lpp for long waves ($\lambda/L = 1.15,\ 1.37$), outlet is placed 1.35 Lpp from the outlet of the domain. The sides, top and bottom of the domain are kept same as calm water simulation. Open FOAM's built in blockMeshDict is used to generate computational domain. To place the hull within the domain snappyHexMeshDict has been used. Multiple refinements are done using six-topoSetDict to capture the free surface and mesh motion. In case of wave simulations multiple refinements are done up to inlet of the domain to avoid wave reflection near the inlet. Three boundary layers are generated over the hull to satisfy y+ criteria. The mesh assembly for calm and wave condition have shown in Fig. 3.

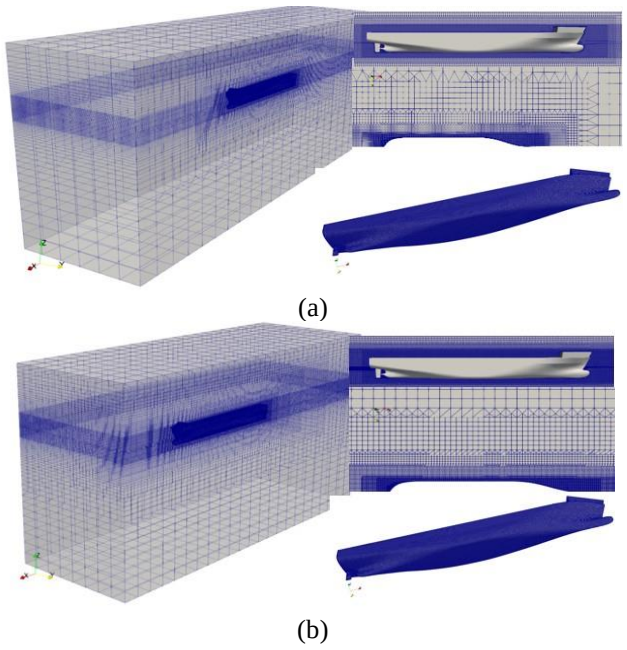

(a)

(b)

Fig.3 General mesh assembly for KCS hull in (a) calm water and (b) wave condition.

8. Wave generation

To generate wave within the domain Open FOAM's waveProperties dictionary is used. The wave is modeled by Stokes II wave. Equation of the Stokes 2nd order wave is giver below in Equation no (3).

$$\eta = \frac{H}{2} COS(\kappa x - \omega t + \phi) + \kappa \frac{H^2}{4} \frac{3-\sigma^2}{4\sigma^3} COS\big(2(\kappa x - \omega t + \varphi)\big) \quad (3)$$

Here, η, H, k, ω, σ, φ, t define modeled wave height, actual wave height, angular wave frequency, radian wave frequency, phase shift, time respectively. The crest of the wave is located at fore perpendicular of the hull. Damping at inlet is done for smooth wave generation.

9. Result & Discussion

The calm water simulation is performed first to evaluate total resistance in calm water at Froude number 0.26. Following that, head wave simulations are run at four different wave lengths $\lambda/L = 0.65, 0.85, 1.15,\ 1.37$ at the same Froude number. All the simulations are run at heave and pitch free motion. A systemic validation and verification study is performed for both calm water and head wave simulations. The verification study is performed for mesh dependency analysis. For head wave simulation a Fourier transformation is performed using MATLAB to reduce noise in the signal and to calculate harmonics. Only 0^{th} harmonic is compared in the present study. Finally, the added resistance coefficient in head waves are calculated and increment in power is predicted. It is clear that with increment in wave lengths and heights there is a sudden increment in total resistance. A resonance is also observed where wave length is close to ship length.

9.1 Calm water simulation

Calm water simulation is performed in model scale at Froude number 0.26 which is corresponding to speed 24 knots in full scale. After SIMMAN 2020 work shop it is mandatory to simulate in calm water with 2 DOF (Heave & Pitch free motion). The numerical results of C_T (Total resistance co-efficient) θ (trim) and σ (sinkage) are validate with experimental result provided by NMRI (National Maritime Research Institute) in Tokyo CFD work shop 2015. Validation study of calm water simulation is mentioned in Table 4.

Table 4 Validation in calm water condition.

Result	$C_T\ (10^{-3})$	$Trim$ (deg)	$Sinkage(Z/Lpp\%)$
EFD	3.835	-0.1646	-2.07x10^{-3}
CFD	3.857	-0.180	-2.46 x10^{-3}
Error	0.573 %	9.35 %	18.84

Total resistance co-efficient show good agreement with experimental result but trim and sinkage shows relatively large error. However absolute difference between them are very small. The reason may be selection of location COG (center of gravity). Actual position of COG is not known value of trim and sinkage obtain from CFD result are 0.18 deg by bow and 14.93 mm which are reasonable for such 6.0702 m model.

9.2 Verification study

For verification study, two most popular methods are used to analyze uncertainties are Grid Convergence Index (GCI) and Correction factor (Ci). The GCI approach described well by Celik et al. [10]. The GCI method estimates uncertainty from grid and time step errors using Richardson extrapolation with multiple solutions on refined grids. Stern et al. [11] proposed Correction factor-based approach. Three different meshes with a constant refinement ratio (1.18) have been used.

Table 5 Verification for calm water.

Parameter	Cell No. (million)	C_T (10^{-3})	Trim (deg)	Sinkage (Z/Lpp %)
Mesh 1 (Fine)	2.00	3.857	-0.18	-2.46
Mesh 2 (Medium)	1.40	3.88	-0.195	-2.51
Mesh 3 (Coarse)	0.90	3.93	-0.20	-2.31
Grid Convergence Index $GCI_{(21)}$	--	0.63	5.21	0.85
Grid Convergence Index $GCI_{(32)}$	--	1.37	1.60	3.32
Corrected Uncertainty $U_{(1C)}$	--	0.55	10.64	2.93
Corrected Uncertainty $U_{(2C)}$	--	1.19	3.27	11.50

Resistance, trim, and sinkage have been considered for the uncertainty estimation as shown in Table 5. The resistance coefficient and sinkage have shown monotonic and oscillatory convergence respectively. In case of trim the simulation shows divergence.

9.3 Head wave simulation

Head wave simulations are run at 4 different wave lengths $\lambda/L = 0.65, 0.85, 1.15, and\ 1.37$ respectively at Froude number 0.26. The simulations are run with heave and pitch free motion up to 20 encountering periods. Details about head wave simulation are mentioned in Table 6.

Table 6 Head wave simulation condition.

Case	C1	C2	C3	C4
λ/L	0.65	0.85	1.15	1.37
$H\ (m)$	0.062	0.078	0.123	0.149
$T_e\ (s)$	0.8775	1.0631	1.2886	1.4800

Here,

$$f_w = \sqrt{\frac{g}{2\pi\lambda}} \tag{4}$$

$$f_e = f_w + \frac{U}{\lambda} \tag{5}$$

$$T_e = \frac{1}{f_e} \tag{6}$$

The parameters ($H, \lambda, f_w, f_e, T_e$) are defined as wave height, wave length, frequency of incident wave, encountering frequency, and encountering period respectively. Ships when moving through the wave the actual period of wave is not its absolute period f_w but the period of wave encountered by the ship depending on the heading of ship. In case of head sea (relative angle between ship heading and wave direction = 180 degree) encountering period will be less than actual period. Time history of C_T (total resistance co-efficient is plotted over one encountering period and compared with experimental results. For making comparison reconstructed Fourier signal has been used.

$$X(t) = \frac{X_0}{2} + \sum_{n=1}^{N} X_n cos(2\pi f_e t + \Delta\gamma_n) \tag{7}$$

where,

$$\Delta\gamma_n = \gamma_n - \gamma_I$$

$$a_n = \frac{2}{T_e}\int_0^{T_e} X(t)cos(2n\pi f_e t)dt\ \ (n = 0,1,2)$$

$$b_n = \frac{2}{T_e}\int_0^{T_e} X(t)sin(2n\pi f_e t)dt\ (n = 1,2)$$

$$X_n = \sqrt{a_n^2 + b_n^2}$$

$$\gamma_n = tan^{-1}(-\frac{a_n}{b_n})$$

Here,

$X_o = 0^{th}$ harmonic amplitude, $X_n = n^{th}$ harmonic amplitude, $a_n, b_n =$ Fourier co-efficient, $\gamma_I =$ initial phase, $\gamma_n =$ nth harmonic phase. At $t/T_e = 0$ the wave crest is at fore perpendicular. The Fouier analysis is done in Matlab R2024 version. Comparison between CFD and EFD signal C_T over one encountering period have been shown in Fig.4.

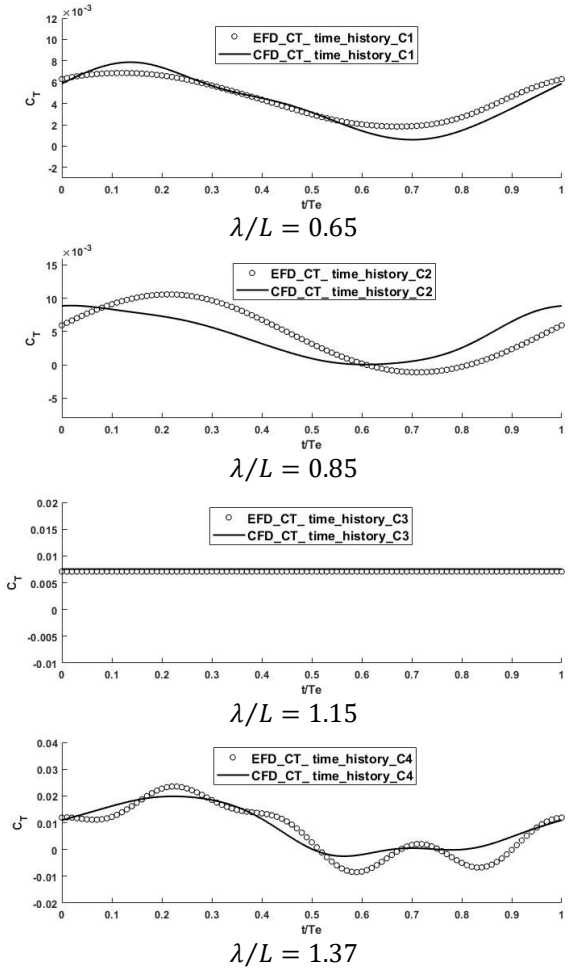

Fig.4 Resistance coefficient at four wave lengths

It is seen that the experimental result shows a close approximation with experimental results except case C2 shown in Fig 4. There is a notable difference between peak and trough values. The reason may be the incapability of the selected turbulence model to adopt higher frequency oscillation and a limited number of Fourier coefficients. In the case of $\lambda/L = 1.15$ only the mean value of the resistance co-efficient is compared due to resonance. Validation of 0th harmonics of C_T for different wavelengths against EFD results is mentioned in Table 7.

Table 7 Validation in wave condition.

Case	C1	C2	C3	C4
EFD C_T	0.008253	0.009244	0.014157	0.0140
CFD C_T	0.0086	0.00877	0.0151	0.0161
Deviation	4.20 %	5.12 %	6.66 %	15 %

Percentage of error increases for longer wave lengths shown in Table 7. The possible reason is mesh density in x and z direction. To improve the results cell no in x and z direction need to be increased.

9.4 Verification study

Similarly, the GCI and Correction-based methods have been used in the wave condition to calculate the uncertainty of the simulation as calm water simulation. The purpose of the uncertainty analysis is to check the dependency of numerical results on mesh. Three different meshes with a refinement ratio (1.18) have been taken into account. Only the 0th harmonic of the resistance coefficient (C_T) is taken for uncertainty analysis shown in Table 8.

Table 8 Verification in wave condition.

Parameter	Cell No. (million)	C_T
Mesh 1 (Fine)	4.5	0.088
Mesh 2 (Medium)	3.1	0.087
Mesh 3 (Coarse)	2.2	0.0875
Grid Convergence Index $GCI_{(21)}$	--	0.0142
Grid Convergence Index $GCI_{(32)}$	--	0.0071
Corrected Uncertainty $U_{(1C)}$	--	1.76%
Corrected Uncertainty $U_{(2C)}$	--	0.08%

9.5 Added resistance prediction

The added resistance is caused by while ship is moving in wave energy from the ship due to its motion is radiated to wave system and diffraction of incident wave on hull. Energy loss from both of the phenomena causes this additional resistance. This is highly dependent on wave length. In the present paper, the added resistance co-efficient for different wave length at Froude no 0.26 which corresponds to 24 knots in full scale is calculated using below equations.

$$R_{AW} = \bar{R}_{wave} - R_{calm} \tag{8}$$

$$C_{AW} = \frac{R_{AW}}{\rho g \zeta^2 B^2 / L} \tag{9}$$

Here,

R_{AW} = Added resistance

R_{wave} = Time average value of resistance in wave over one encountering period in wave

R_{Calm} = Calm water resistance

C_{AW} = Added resistance co-efficient

g = Gravitational acceleration

ζ = Wave amplitude ($\frac{H}{2}$)

B = Beam of ship

L = Length between perpendiculars

The added resistance co-efficient is plotted in below in Fig.5 against different ship to wave length ratios.

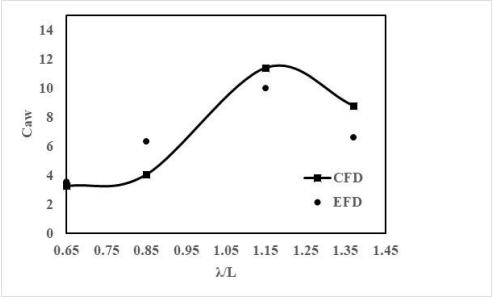

Fig.5 Added resistance coefficient against wave lengths

The added resistance co-efficient is over predicted except case C-2. The result can be improved by increasing mesh resolution. Percentage of increase in resistance are plotted against wave to ship length ratios shown in Fig 6.

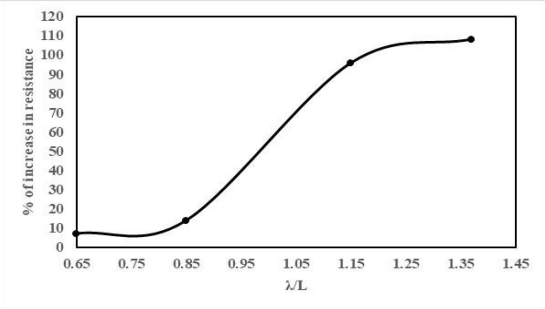

Fig.6 Percentage of increment in resistance against wave lengths

The increments in resistance are within 15-20% in short wave lengths up to $\lambda/L = 0.85$, but in case of higher wave lengths, it is almost twice.

10. Conclusion

In this paper the additional resistance overcome by a ship in a sea way is predicted. The study begins with prediction of calm water resistance. In case of calm water simulation, CFD results shows very good approximation with experimental results. After performing verification and validation study in calm water head wave simulations are performed. For verification study only 0^{th} harmonic of

Four different wave lengths $\lambda/L = 0.65, 0.85, 1.15, 1.37$ with changing wave height are considered here. Time history of total resistance co-efficient C_T shows reasonable accuracy but leaves a scope for improvement. Although the numerical uncertainty is within limit. However, it is not possible to model the actual wave condition as in towing tank by means of mathematical modeling of wave via simulations.

The added resistance co-efficient is predicted at Froude number 0.26 which corresponds to design speed 24 knots. The maximum added resistance occurs at $\lambda/L = 1.15$ where the wave length is close to ship length. In this region the natural frequency of motion is close to encountering frequency of wave. So, the motion becomes rigorous. The added resistance is almost close to twice of resistance in calm water. Resonance should always be avoided for habitability and overloading of engine.

The method used in the present study is useful to calculate resistance and motion response in sea way. The CFD results of C_T are close to experimental results. The added resistance co-efficient are over predicted in most of the case which may be due to limited cells number in x and z direction. Finally, the study concludes with prediction of added resistance co-efficient and increase in resistance with wavelengths which may be useful for estimating sea margin. A future recommendation of the study is to do analysis of motion in head waves.

References

[1] Equasis, The world merchant fleet, European Maritime Safety Agency, 2020.

[2] Havelock, T., H., and F.R.S, The Resistance of a Ship among Waves, 1937.

[3] Maruo, H., the Drift of a Body Floating on Waves, *Journal of SHIP RESEARCH,* 1960 .

[4] Gerritsma, P., J., and Beulielman, W., ANALYSIS OF THE RESISTANCE INCREASE I N WAVES OF A FAST CARGO SHIP, 1971.

[5] Orihara, H., and Miyata, H., Evaluation of added resistance in regular incident waves by computational fluid dynamics motion simulation using an overlapping grid system, *Journal of MARINE SCIENCE AND TECHNOLOGY*, vol. 8, pp. 47-60, 2003 .

[6] Hafizul Islam, H., Rahaman, M., Islam, M., R., and Akimoto, H., Application of a RaNS and PF-Based Method to Study the Resistance and Motion of a Bulk Carrier, *Journal of Marine Science and Technology*, 2018..

[7] H. Islam, H., and Soares, C.,G., Predicting head wave resistance for a KVLCC2 model using OpenFOAM, in *maritime Technology and Engineering*, 2021, p. 9.

[8] Hong Quang Nguyen, H., Q., and Vu, H., K., Numerical Simulation of Ship Sailing In Regular Head Waves Using CFD Method, *International Journal of Mechanical Engineering and Robotics Research*, vol. 10, no. 4, pp. 183-188, 2021.

[9] Ping-Chen Wu, P., C., Hossain, M., A., Kyaw, H., A., Ayaka Matsumoto and Yasuyuki Toda, Forces, Ship Motions and Nominal Wake for KCS Ship Model in Regular Head Waves, in *International Ocean and Polar Engineering Conference (ISOPE)* , Sapporo, Japan, 2018.

[10] Celik, I., U. Ghia, U., Roache, P., J., Freitas, C., J., Coloman, H., and Raad, P., E., Procedure for Estimation and Peporting of Uncertainty Due to Descretization in CFD Applications, *Journal of Fluids Engineering*, vol. 130, no. 7, p. 078001(4 pages), 2008.

[11] Stern, F., Wilson, R., and Shao, J., Quantitive V&V of CFD simulations and certifications of CFD codes, *INTERNATIONAL JOURNAL FOR NUMERICAL METHODS IN FLUIDS*, vol. 50, no. 11, pp. 1335-1355, 2006